

(1952).

<sup>10</sup>A. L. Jain and S. H. Koenig, Phys. Rev. 127, 442 (1962).

<sup>11</sup>R. N. Bhargava, Phys. Rev. 156, 785 (1967).

<sup>12</sup>L. S. Lerner, Phys. Rev. 127, 1480 (1962).

<sup>13</sup>L. S. Lerner, Phys. Rev. 130, 605 (1963).

<sup>14</sup>Y. Eckstein and J. B. Ketterson, Phys. Rev. 137, A1777 (1965).

<sup>15</sup>R. J. Balcombe and A. M. Forrest, Phys. Rev. 151, 550 (1966).

<sup>16</sup>R. D. Brown, Bull. Am. Phys. Soc. 13, 44 (1968).

<sup>17</sup>R. D. Brown, Bull. Am. Phys. Soc. 9, 264 (1964).

<sup>18</sup>R. D. Brown, IBM J. Res. Develop. 10, 462 (1966).

<sup>19</sup>A. H. Kahn and H. P. R. Frederikse, Solid State Phys. 9, 257 (1959).

<sup>20</sup>E. N. Adams and T. D. Holstein, J. Phys. Chem. Solids 10, 254 (1959).

<sup>21</sup>R. Kubo, S. J. Miyake, and N. Hashitsume, Solid State Phys. 17, 269 (1965).

<sup>22</sup>L. M. Roth and P. N. Argyres, Semicond. Semimet. 1, 159 (1966).

<sup>23</sup>Comprehensive lists of references to previous work are contained in Refs. 19-22.

<sup>24</sup>S. J. Miyake, thesis, Tokyo University, 1962 (unpublished).

<sup>25</sup>An obvious error in Kubo's result has been corrected in Eq. (3). Equation (76) in Ref. 22 also contains errors.

<sup>26</sup>R. B. Dingle, Proc. Roy. Soc. (London) A211, 500 (1952).

<sup>27</sup>B. Davydov and I. Pomeranchuk, J. Phys. (USSR) 2, 147 (1940).

<sup>28</sup>W. S. Boyle and G. E. Smith, Progr. Semicond. 7, 1 (1963).

<sup>29</sup>R. D. Brown, R. L. Hartman, and S. H. Koenig, Phys. Rev. 172, 598 (1968).

<sup>30</sup>G. A. Williams, Phys. Rev. 139, A771 (1965).

<sup>31</sup>G. E. Smith, G. A. Baraoff, and J. M. Rowell, Phys. Rev. 135, A1118 (1964).

<sup>32</sup>J. Ketterson and Y. Eckstein, Phys. Rev. 132, 1885 (1963).

<sup>33</sup>R. N. Dexter (private communication). Professor Dexter informed me that these periods had been seen in the course of investigations of the dHvA effect in uniaxially stressed bismuth [F. F. Huppe, thesis, University of Wisconsin, 1966 (unpublished)] and were being studied further by A. B. Holland. Huppe had measured approximately the same period, with the same effective mass, along the trigonal and was able to follow it further in angle in the binary plane where it fell off quite rapidly, and in fact, passed approximately through the  $x$  points in Fig. 4. These periods remained unexplained. However, Dexter speculated that they were due to imperfections in the sample.

<sup>34</sup>A. B. Holland (private communication). Holland independently determined that these periods were associated with inelastic strain and showed from x-ray data that they were due to twinning, confirming Dexter's earlier speculation.

<sup>35</sup>E. O. Hall, *Twinning* (Butterworths, London, 1961), p. 83.

<sup>36</sup>See Ref. 11, Table I, for a list of periods reported by other investigators.

<sup>37</sup>B. Lax, Bull. Am. Phys. Soc. 5, 167 (1960); B. Lax, J. G. Mavroides, H. J. Zieger, and R. J. Noyes, Phys. Rev. Letters 5, 241 (1960).

<sup>38</sup>R. L. Hartman, Phys. Rev. 181, 1070 (1969).

<sup>39</sup>W. S. Boyle and A. D. Brailsford, Phys. Rev. 120, 1943 (1960).

<sup>40</sup>D. H. Brownell and E. H. Hygh, Phys. Rev. 164, 909 (1967).

## Optical Constants of Disordered Binary Alloys: Intraband Transitions in the Coherent-Potential Approximation\*

B. Velicky<sup>†</sup> and K. Levin

Division of Engineering and Applied Physics, Harvard University, Cambridge, Massachusetts 02138

(Received 15 January 1970)

The optical constants of disordered binary alloys  $A_xB_{1-x}$  have been computed in the coherent-potential approximation for all frequencies, all  $x$ , and all reasonable scattering strengths, using a simple one-band model. Our results are compared with the classical Drude formula, and deviations are found stemming from critical points and the effects of alloying. In addition, the high-frequency behavior is shown to be dependent on the concentration  $x$  and scattering strength in the alloy.

### I. INTRODUCTION

In the present paper the frequency-dependent conductivity  $\sigma(\omega)$  of random binary alloys is calculated for all frequencies, all impurity concen-

trations, and a wide range of alloy scattering strengths. The coherent-potential approximation (CPA) is applied to the Kubo formula<sup>1</sup> for the complex frequency-dependent conductivity. This approximation has been shown<sup>2,3</sup> to lead to easily

calculable expressions for the one-electron Green's function and the static conductivity when a short-range-scattering single-band-model Hamiltonian is used. It reduces to the rigid-band and dilute-alloy limits for the appropriate choice of alloy parameters and is applicable to arbitrary band shapes.

The frequency dependence of the conductivity has been discussed by numerous authors. The classical Boltzmann equation was shown to be invalid<sup>4</sup> for frequencies large compared with the inverse lifetime  $\tau^{-1}$  of the current carriers. In addition, it places a restriction on the allowed magnitude of the carrier lifetime. Both these limitations can be circumvented by using quantum-mechanical approaches which have, thus far, been applied to determine the high- and low-frequency limits of the conductivity.<sup>5,6</sup> In Ref. 5 the high-frequency conductivity was calculated for a system of free electrons with dilute impurities. In Ref. 6 the case of very low and very high frequencies was treated for arbitrary dispersion laws but as a second-order expansion in the impurity potential. It is felt that the present calculation will provide a more complete treatment of the frequency-dependent conductivity, for our results are not restricted to specific frequency regions, alloy scattering strengths, concentrations, or band shapes. In contrast to the work of others, as a consequence of the short range of the impurity potential, we are able to obtain workable expressions for the conductivity which can be numerically evaluated.

Our attention will be focussed on obtaining useful results, and we shall not discuss, in detail, the nature and validity of the CPA. We shall, however, demonstrate its consistency when applied to  $\sigma(\omega)$  by showing that it leads to correct analytic behavior in the conductivity and therefore to an  $f$ -sum rule simply related to its high-frequency behavior. It was shown previously<sup>2,3</sup> that both the single-particle Green's function and the (two-particle) response function behave appropriately in the high-frequency limit within the CPA.

In Sec. II the classical Drude formula for the conductivity will be discussed. For comparative purposes, particular attention will be given to its high- and low-frequency behavior and the  $f$ -sum rule it satisfies. It is emphasized here that the effective number of carriers per unit volume  $n$  is independent of impurity concentration  $x$  and the strength of the scattering potential. The restrictions on the validity of the Drude formula are given explicitly. The CPA is briefly described and the Kubo formula introduced.

In Sec. III we discuss the results of the CPA applied to the Kubo formula for large  $\omega$ . It is shown that while the high-frequency behavior of

the imaginary part of the conductivity is very similar to that obtained from the Drude formula, the absorptive part of the conductivity is, as expected, zero for these frequencies. The  $f$ -sum rule is used to define a quantity  $n_1$  the effective number of carriers in analogy with  $n$  in the Boltzmann equation.

In Sec. IV the absorptive part of the conductivity is discussed for frequencies which are very low and for those which are comparable to the bandwidth. It is shown that at frequencies coinciding with energies of band singularities, e.g., critical points, measured relative to the Fermi level, sharp structure appears in the real part of  $\sigma(\omega)$ . For a range of frequencies which may lie outside the limits of validity of the Boltzmann equation, a quasi-Drude formula is shown to be satisfied when the Fermi energy is in a smooth part of the band.

In Sec. V numerical examples for a simple cubic tight-binding band will be given of two experimentally important quantities: the real part of the conductivity and the effective carrier number  $n_1$ . The latter is plotted as a function of impurity concentration  $x$ , and it is demonstrated that it is significantly  $x$  dependent for scattering strengths comparable to those in ordinary metallic alloys. Consequently, high-frequency behavior is affected by alloying. The absorptive part of  $\sigma$  is discussed as a function of frequency, and it is demonstrated that not only is it dependent on the choice of alloy parameters, but it also reflects strongly critical points, band edges, and other sharp structure in the band.

## II. COMPLEX CONDUCTIVITY: BOLTZMANN AND KUBO FORMULAS

We begin with a brief review of the two formal expressions for the conductivity obtained from the transport equation<sup>4</sup> and the Kubo formula.<sup>1</sup> The second and more general of these two will be used here to calculate the conductivity. Because it is difficult to evaluate the conductivity for a random alloy exactly, we shall apply to the Kubo formula an approximation called the coherent-potential approximation (CPA). The details of this approximation are fully discussed in Refs. 2 and 3. In the interest of keeping this section of reasonable length, however, we shall merely quote from these two references the results that are used here.

We adopt the same Hamiltonian for the electrons in the alloy  $A_xB_{1-x}$  as was done in Refs. 2 and 3. It has a single band. Its diagonal elements (atomic levels)  $\epsilon_i$  in the Wannier representation may assume one of two possible values  $\epsilon^A$  or  $\epsilon^B$  corresponding to the type of atom at site  $i$ , and its off-diagonal elements are independent of alloying:

$$H = W + D = \sum' |i\rangle b_{ij} \langle j| + \sum |i\rangle \epsilon_i \langle i| . \quad (1)$$

Here  $W$  is diagonal in the Bloch basis corresponding to the pure crystal

$$W = \sum |k\rangle \epsilon(k) \langle k| . \quad (2)$$

The crystal velocity operator is<sup>7</sup>

$$\hat{v} = \sum |k\rangle v(k) \langle k| = \sum |k\rangle \nabla_k \epsilon(k) \langle k| . \quad (3)$$

For a fixed electron concentration per site  $c$  and absolute temperature  $\beta^{-1}$ , the equilibrium one-electron density matrix for the alloy is

$$\rho = f(H) = (1 + e^{\beta(H-\mu)})^{-1}, \quad \beta = k_B T \quad (4)$$

where  $\mu$  is given by

$$\text{Tr}\rho = cN. \quad (5)$$

Equivalently, Eq. (5) can be written

$$\int d\eta g(\eta) f(\eta) = c, \quad (5')$$

where  $g(\eta)$  is the density of states per site.

The complex conductivity tensor  $\sigma(\omega)$  is defined by

$$j = \sigma(\omega)E = [\sigma'(\omega) + i\sigma''(\omega)]E, \quad (6)$$

where  $j$  is the induced current density and

$$E = E_0 e^{-i\omega t} \quad (7)$$

is the electric vector of the incident light wave of frequency  $\omega$ . We adopt the dipole approximation; consequently,  $\sigma$  is independent of wave vector.

From the Boltzmann equation, an expression for  $\sigma^{\alpha\beta}(\omega)$  formally resembling the classical Drude formula can be obtained<sup>4</sup> where

$$\sigma^{\alpha\beta}(\omega) = (n^{\alpha\beta} e^2 / m) (\tau^{-1} - i\omega)^{-1}, \quad (8)$$

$$\sigma^{\alpha\beta}(\omega) = (n^{\alpha\beta} e^2 / m) [\tau^{-1}(\tau^{-2} + \omega^2)^{-1} + i\omega(\tau^{-2} + \omega^2)^{-1}]. \quad (8')$$

Here  $\tau$  is the transport relaxation time and  $n$  is the effective number of carriers,  $m$  is the electron mass, and  $e$  is the electric charge.

The Drude formula has, generally speaking, two types of properties, those which characterize the behavior of complex conductivities, in general, and those specific to the model assumed and the approximations involved. The first category of properties may be summarized as follows<sup>1</sup>: (a) The absorptive part of the conductivity  $\sigma'$  is positive for all  $\omega$ . (b) The crossing symmetry

$$\sigma(\omega) = \sigma^*(-\omega) \quad (9)$$

is obeyed, so that  $\sigma'$  is even in  $\omega$ . (c)  $\sigma(\omega)$  has an analytic continuation into the upper half-plane and a zero of the first order at infinity; therefore, it satisfies the Kramers-Kronig relations. (d) For infinitesimal damping  $\tau \rightarrow \infty$ , Eq. (8) reduces to

$$\sigma(\omega) = (ne^2/m)[\pi\delta(\omega) + i\omega^{-1}]. \quad (10)$$

Of the second class of properties, the most salient, perhaps, is that the Drude formula [Eq. (8)] depends only on two parameters  $n$  and  $\tau$ . Consequently, it contains only one characteristic frequency  $\tau^{-1}$ ; there is no additional energy characterizing, for example, the band structure. The low- and high-frequency regions are defined by the magnitude of  $\omega\tau$  relative to one. In these regions Eq. (8) reduces to

$$\sigma(0) = ne^2\tau/m, \quad \omega\tau \ll 1 \quad (11)$$

and

$$\sigma(\omega) \approx ine^2/m\omega + ne^2/m\tau\omega^2 + \dots, \quad \omega\tau \gg 1. \quad (12)$$

Finally a sum rule may be obtained either directly or from Eq. (12) and property (c):

$$\int_0^\infty \sigma'(\omega) d\omega = \pi ne^2/2m. \quad (13)$$

These last three equations will shortly be compared with their CPA counterparts.

The Boltzmann equation yields the following microscopic expressions for  $n$  and  $\tau$  for a system of volume  $\Omega$ :

$$n^{\alpha\beta}/m = \Omega^{-1} \text{Tr} f^0(W) \frac{\partial^2 W}{\partial k^\alpha \partial k^\beta}, \quad (14)$$

and at  $T=0$  for a weakly scattering alloy<sup>8</sup>

$$\tau^{-1} = 2\pi x(1-x)(\epsilon^A - \epsilon^B)^2 g^0(\mu^0), \quad (15)$$

where  $f^0(W)$  is the equilibrium distribution function corresponding to the pure crystal with  $\epsilon^A = \epsilon^B = 0$  and electron concentration  $c$ . Here  $g^0(E)$  denotes the density of states in the pure crystal and  $\mu^0$  is the Fermi level. Two important statements can be made about these equations;  $n$  is dependent only on the pure-crystal properties and  $\tau^{-1}$  involves the "Nordheim" concentration dependence<sup>9</sup>  $x(1-x)$  and the Fermi level of the pure crystal  $\mu^0$  only.

There are two restrictions on the validity of the use of a transport equation to determine  $\sigma(\omega)$ . These are

$$\omega\tau \ll 1 \quad (16)$$

and

$$|\mu^0 - E_c| \tau \gg 1, \quad (17)$$

where  $E_c$  is the energy of the nearest critical point in the band. The first of these states that there must be many collisions during a single period  $2\pi/\omega$ . The second is just the Landau-Peierls condition,<sup>10</sup> which states that the scattering must be weak enough so that the broadening of the band levels due to scattering should be negligible. The restriction on the Boltzmann equation expressed in Eq. (16) is frequently ignored. Deviations from Eq. (8) when  $\omega\tau \gg 1$  have been found for weakly scattering alloys<sup>6</sup> and dilute alloys<sup>5</sup> using quantum-mechanical methods. It is the

purpose of the Sec. III to derive the conductivity for all  $\omega$  not subject to the restriction of Eq. (16) nor to Eq. (17), i.e., the weak-scattering and the dilute-alloy limits. Because the CPA is applicable outside these limits of dilute- and weakly-scattering alloys, it enables us to treat more general alloy systems than in previous theories and to thus calculate the conductivity for a wide range of scattering strengths and for all impurity concentrations and frequencies. We adopt the Kubo formula<sup>1</sup> as a starting point to which we shall apply our approximation.

To this end, we introduce the resolvent (Green's function)

$$G(z) = (z - H)^{-1} \quad (18)$$

into the Kubo formula and obtain an exact expression for the configuration averaged conductivity,

$$\begin{aligned} \sigma^{\alpha\beta}(\omega) = & \frac{ie^2}{\pi\Omega\omega} \int d\eta f(\eta) \left[ \text{Tr} \left( \langle G''(\eta - i\omega) \rangle \frac{\partial^2 W}{\partial k^\alpha \partial k^\beta} \right) \right. \\ & + \text{Tr} \langle G''(\eta - i\omega) \hat{v}^\alpha G(\eta + \omega + i\omega) \hat{v}^\beta \rangle \\ & \left. + G(\eta - \omega - i\omega) \hat{v}^\alpha G''(\eta - i\omega) \hat{v}^\beta \right], \end{aligned} \quad (19)$$

where  $\langle \dots \rangle$  denotes the average over-all alloy configurations having an impurity concentration  $x$ .

The CPA<sup>2,3</sup> is easily applied to Eq. (19). Briefly, the CPA is a self-consistent single-site approximation which makes it possible to determine a configuration average of the multiple-scattering expansion of  $G$ . When an electron scatters from a given site, the random surroundings of the site are approximated by the averaged effective medium. The results of this approximation for the model Hamiltonian given by Eq. (1) can be summarized as follows:

$$\langle G \rangle = \sum_k |k\rangle \overline{G}_k(z) \langle k|, \quad (20)$$

$$\overline{G}_k(z) = [z - \epsilon(k) - \Sigma(z)]^{-1}, \quad (21)$$

$$\begin{aligned} \langle G(z_1) \hat{v}^\alpha G(z_2) \rangle = & \langle G \rangle \hat{v}^\alpha \langle G \rangle = \sum_k |k\rangle \overline{G}_k(z_1) v_k^\alpha \\ & \times \overline{G}_k(z_2) \langle k|, \end{aligned} \quad (22)$$

where  $\langle G \rangle$  is the configuration average of  $G$ . Equation (20) shows that the averaged Green's function is diagonal in the Bloch basis.<sup>2,11</sup> Equation (21) defines the self-energy  $\Sigma(z)$  which is  $k$  independent in the CPA.<sup>2,11</sup> Equation (22) shows that the result of the CPA two-particle decoupling is to replace the average of  $GvG$  by the product of the averages.<sup>3</sup> Both the  $k$  independence of  $\Sigma$  and the factorization in Eq. (22) are direct consequences of applying a single-site approximation to a Hamiltonian whose atomic-scattering potentials have a short range.

The self-energy is given, for Eq. (1), by Soven's

equation<sup>11</sup>

$$\Sigma(z) = \epsilon - (\epsilon^A - \Sigma) F^0[z - \Sigma(z)] (\epsilon^B - \Sigma), \quad (23)$$

where  $\bar{\epsilon} = x\epsilon^A + (1-x)\epsilon^B$  is the virtual-crystal atomic level, and  $F^0$  is defined in terms of  $g^0(\eta)$  the pure-crystal ( $\epsilon^A = \epsilon^B = 0$ ) density of states per atom as

$$F^0(z) = \int d\eta (\eta - z)^{-1} g^0(\eta). \quad (24)$$

In the CPA,

$$g(\eta) = \pm \pi^{-1} \text{Im} F^0[\eta \mp i\omega - \Sigma(\eta \mp i\omega)] \quad (25)$$

is the average density of sites per atom in the alloy. This quantity will be used to determine the Fermi energy from Eq. (5').

### III. CPA EXPRESSION FOR $\sigma(\omega)$ HIGH-FREQUENCY BEHAVIOR

To obtain  $\sigma(\omega)$  in the CPA, we use Eqs. (20) and (22) in (19) and assume, for simplicity, that the pure crystals have cubic symmetry. Then, in this approximation,

$$\sigma(\omega) = (ie^2/\omega) [n_1/m + Y(\omega)], \quad (26)$$

where

$$\frac{n_1}{m} = (\pi\Omega)^{-1} \int d\eta f(\eta) \sum_k \text{Im} \overline{G}_k(\eta - i\omega) \frac{\partial^2 \epsilon(k)}{\partial k^\alpha \partial k^\alpha} \quad (27)$$

and

$$\begin{aligned} Y(\omega) = & (\pi\Omega)^{-1} \int d\eta f(\eta) \sum_k [v^\alpha(k)]^2 [\overline{G}_k(\eta + \omega + i\omega) \\ & + \overline{G}_k(\eta - \omega - i\omega)] \text{Im} \overline{G}_k(\eta - i\omega). \end{aligned} \quad (28)$$

We shall now check properties (a)–(d) quoted in Sec. II and obtain expressions to replace Eqs. (12)–(14). That  $\sigma(\omega)$  satisfies the general properties of complex conductivities follows easily from Eq. (26) and from the equations

$$Y(0) = -n_1/m, \quad (29)$$

$$Y(\omega) = \mathcal{O}(\omega^{-2}). \quad (30)$$

Equation (29) states that  $\sigma(\omega)$  is well behaved at  $\omega = 0$ . Equation (30) shows that as  $\omega \rightarrow \infty$ ,  $\sigma(\omega) \rightarrow 0$  as  $1/\omega$ . Equation (29) follows from Eqs. (21) and (26). To prove Eq. (30), we use the fact that  $\Sigma(\omega) \rightarrow \bar{\epsilon}$  as  $\omega \rightarrow \infty$ , obtained from Eq. (23).

From Eq. (30), it follows that  $\sigma(\omega)$  behaves at high frequencies as

$$\sigma(\omega) = in_1 e^2 / m\omega + \mathcal{O}(\omega^{-3}). \quad (31)$$

In conjunction with the Kramers-Kronig relations, Eq. (31) implies the sum rule

$$\int_0^\infty \sigma'(\omega) d\omega = \pi n_1 e^2 / 2m. \quad (32)$$

By comparing Eqs. (31) and (12), it is clear that

the high-frequency behavior of  $\sigma''(\omega)$  is very similar in both cases and suggests that one should identify  $n_1$  with the effective number of carriers in the CPA conductivity. The sum rules, Eqs. (32) and (13), are also of a similar form. Equation (32) coincides with the exact sum rule<sup>1</sup> evaluated in the CPA only when  $n_1$  is given by Eq. (27). In contrast to the behavior of  $\sigma''(\omega)$  at high frequencies,  $\sigma''(\omega)$  is not at all Drude-like and becomes identically zero for sufficiently high frequencies, which will be discussed shortly.

To understand the relation between the two effective carrier numbers, Eqs. (27) and (14), it is convenient to write them in a similar form. Introducing a function  $\phi(z)$ , which depends only on the pure crystal ( $\epsilon^A = \epsilon^B = 0$ ) properties,

$$\phi(z) = m\Omega^{-1} \sum_k [z - \epsilon(k)]^{-1} \frac{\partial^2 \epsilon}{\partial k^\alpha \partial k^\alpha}, \quad (33)$$

these two equations may be rewritten as

$$n = \pi^{-1} \int d\eta f^0(\eta) \phi''(\eta - i\omega) \quad (34)$$

and

$$n_1 = \pi^{-1} \int d\eta f(\eta) \phi''[\eta - \Sigma(\eta - i\omega)], \quad (35)$$

where we have used the fact that  $\Sigma$  is  $k$  independent in this last equation. While  $n$  is independent of alloying,  $n_1$  is not because of its explicit dependence on  $\Sigma$  in the argument of  $\phi''$ . The shift in the Fermi energy owing to alloying is represented by the function  $f(\eta)$  [rather than  $f^0(\eta)$ ], and it may be seen from Eqs. (5') and (25) that this shift is obtained by an energy renormalization identical to that appearing in the argument of  $\phi''$ . Only in the virtual-crystal limit does  $n_1$  reduce to  $n$ . In this case both the Fermi energy and the argument of  $\phi''$  are shifted by the same constant amount  $\bar{\epsilon}$ .

#### IV. FREQUENCY DEPENDENCE OF THE REAL PART OF THE CONDUCTIVITY FOR $T = 0$

Up to now, comparisons with the Drude formula and the CPA conductivity have been relatively simple, primarily because the high-frequency properties just examined did not involve the parameter  $\tau$ , or, equivalently, the function  $Y(\omega)$ . To understand the finer details of Eq. (26), it is convenient to look only at  $\text{Re}\sigma(\omega)$ ; Kramers-Kronig transforms may be performed on  $\text{Re}\sigma(\omega)$  to determine  $\text{Im}\sigma(\omega)$ .

Equation (26) may be easily evaluated at  $T = 0$  by integrating over the Brillouin zone in a manner similar to that used to obtain Eq. (35). Using the identity

$$\begin{aligned} \bar{G}_k(z_1) \bar{G}_k(z_2) &= [z_2 - z_1 + \Sigma(z_1) - \Sigma(z_2)]^{-1} \\ &\times [\bar{G}_k(z_1) - \bar{G}_k(z_2)], \end{aligned} \quad (36)$$

and introducing

$$\Phi(z) = \Omega^{-1} \sum_k [z - \epsilon(k)]^{-1} [v^\alpha(k)]^2, \quad (37)$$

which depends only on the properties of the pure crystal with  $\epsilon^A = \epsilon^B = 0$ ,<sup>12</sup> one finds that

$$\begin{aligned} \sigma'(\omega) &= \frac{e^2}{2\pi} \text{Re} \int_{\mu - \omega}^{\mu} d\eta \omega^{-1} \\ &\times \left( \frac{\Phi(\eta + \omega - \Sigma(\eta - \omega)) - \Phi(\eta - \Sigma(\eta - \omega))}{\omega - \Sigma(\eta - \omega) + \Sigma(\eta - \omega)} \right. \\ &\left. - \frac{\Phi(\eta + \omega - \Sigma(\eta + \omega)) - \Phi(\eta - \Sigma(\eta + \omega))}{\omega - \Sigma(\eta + \omega) + \Sigma(\eta + \omega)} \right). \end{aligned} \quad (38)$$

The entire dependence of  $\sigma'(\omega)$  on the band structure appears in the functions  $\Phi(z)$  and  $F^0(z)$ . The latter function determines both  $\Sigma(z)$  and the Fermi energy  $\mu$  as Eqs. (23) and (25) show. The effects of alloying are contained in the function  $\Sigma(z)$ . In order to investigate several special cases of Eq. (38), we shall assume throughout the discussion that the scattering strength  $|\epsilon^A - \epsilon^B|$  is small enough so that the band does not split and, for all energies,  $|\Sigma - \bar{\epsilon}|$  is sufficiently less than the bandwidth. This condition incorporates, but is not restricted to, the dilute-alloy and rigid-band limits. Under various conditions on the frequency we shall see when  $\sigma'(\omega)$  will assume simplified forms and when general statements can be made characterizing its behavior.

Equation (16) states that the low- and high-frequency behavior of the Drude formula obtain when  $\omega\tau < 1$  and  $\omega\tau > 1$ , respectively. Assuming that  $|\Sigma''|^{-1}$  plays the role of a relaxation time  $\tau$ , this suggests that one investigate Eq. (38) when

$$\omega [\max |\Sigma''(E - i\omega)|]^{-1} \gg 1 \quad (39)$$

$$\text{and } \omega [\max |\Sigma''(E - i\omega)|]^{-1} \ll 1. \quad (39')$$

When (39') is satisfied, one obtains<sup>3</sup>

$$\begin{aligned} \sigma'(0) &= |2\Sigma''(\mu)|^{-1} (e^2/\pi) \\ &\times \left( \Phi'' - \Sigma''(\mu) \frac{\partial \Phi}{\partial z} \right|_{\mu - \Sigma(\mu)}, \end{aligned} \quad (40)$$

and when Eq. (39) holds,

$$\begin{aligned} \sigma'(\omega) &= \frac{e^2}{\pi\omega^2} \int_{\mu - \omega}^{\mu} d\eta \omega^{-1} \{ 2\Sigma''(\eta) \Phi''[\eta + \omega - \Sigma(\eta - \omega)] \\ &+ 2\Sigma''(\eta - \omega) \Phi''[\eta - \Sigma(\eta - \omega)] \} + \mathcal{O}(\omega^{-4}). \end{aligned} \quad (41)$$

Equation (40) shows by comparison with the static conductivity  $ne^2\tau/m$  the quantity to be associated with  $\tau^{-1}$  is  $|2\Sigma''(\mu)|$ . This is an exact result, in the weak-scattering limit, as seen by comparison of Eqs. (15) and (23).

Equation (41) also may be given a simple phys-

ical interpretation in the weak-scattering limit. It may be viewed as a result of second-order perturbation theory in the impurity-scattering potential. The initial and final states, characterizing the indirect transitions, have an energy difference  $\omega$  supplied by the electric field and a quasimomentum difference supplied by the random-alloy potential. Equation (41) extends the exact perturbation theoretic result by shifting the argument of  $\Phi$  by an amount  $\Sigma$  the CPA self-energy. Thus it describes indirect transitions, aided by the random-alloy potential, between dressed Bloch states having self-energy  $\Sigma$ .

In general, very little can be said about the frequency dependence of Eq. (41). The high-frequency condition expressed in Eq. (39) does not simplify  $\sigma'(\omega)$  appreciably or make it easily interpretable. To understand the finer details of Eq. (38), it will be of interest to look at specific frequencies, in particular those which coincide with characteristic band energies. Two types of energies will be considered —  $E_c$  the energy of band singularities like critical points, and energies denoting the upper and lower limits, respectively, of the CPA band,  $E_{\max}$  and  $E_{\min}$ . As seen from Eq. (38), or more easily from Eq. (41),  $\sigma'(\omega)$  is determined by the values of  $\Sigma(z)$  and  $\Phi[z - \Sigma(z)]$  for  $z$  such that  $|z - \mu| < \omega$ . A singularity in either  $\Phi$  or  $\Sigma$  at some energy  $E_c$  will be reflected as a singularity in  $\sigma'(\omega)$  at frequencies  $\omega = |E_c - \mu|$ . These singularities are expected to give deviations in  $\sigma'(\omega)$  from Drudelike behavior if  $\omega$  is larger than the smallest value assumed by  $|\mu - E_c|$ , where  $E_c$  may range over all the singularities in the band. When  $\omega$  is equal to  $E_{\max} - E_{\min}$ , another very general statement can be made about  $\sigma'(\omega)$ . Because  $\Sigma'' = \Phi'' = 0$  for  $\omega > E_{\max}$  or  $\omega < E_{\min}$ , it follows that  $\sigma'(\omega) = 0$  for  $\omega > E_{\max} - E_{\min}$ . At these frequencies, the absorption will terminate as expected physically in a one-band system. This cutoff is not implied by Eq. (8), which gives a finite  $\sigma'(\omega)$  for large frequencies. Consequently, the Drude formula is not expected to correctly represent  $\sigma'(\omega)$  at frequencies comparable to the bandwidth. In contrast, however, it should be recalled from Sec. III that in the CPA,  $\sigma'(\omega)$  does behave according to the Drude high-frequency limit Eq. (12).

In the remainder of Sec. IV, we shall investigate under what circumstances a simple Drude formula can be obtained for a limited frequency range using Eq. (38). In Sec. V we shall illustrate our results with numerical examples. We assume here that the Fermi level lies in a smooth part of the band and consider frequencies  $\omega < \omega_m$ . Because  $\Phi$  and  $\Sigma$  are slowly varying, they may be written

$$\Phi[z - \Sigma(z)] = (\Phi' \mp i\Phi'' \operatorname{sgn} z) + (\Psi' \mp i\Psi'' \operatorname{sgn} z)(z - \mu) \quad (42a)$$

$$\text{and } \Sigma(z) = (\Sigma' \mp i\Sigma'' \operatorname{sgn} z) + (\theta' \mp i\theta'' \operatorname{sgn} z)(z - \mu), \quad (42b)$$

$$\text{for } |z - \mu| \leq \omega_m. \quad (43)$$

The constants  $\Phi$ ,  $\Psi$ ,  $\Sigma$ ,  $\theta$  are the values and derivatives of  $\Phi[z - \Sigma(z)]$  and  $\Sigma(z)$  at  $z = \mu$ . The integrations in Eq. (38) may be easily performed. Making additional assumptions that

$$|\theta''| \ll 1 \quad (44)$$

$$\text{and } |\theta'| < 1, \quad (44')$$

i.e., that  $\Sigma''$  vary slowly over the interval  $(\mu - \omega_m, \mu + \omega_m)$ , it follows for frequencies less than  $\omega_m$ , that

$$\sigma'(\omega) = \sigma(0) [\Delta^2 / (\omega^2 + \Delta^2)] (1 + \frac{1}{3}a) \{1 - \frac{2}{3}a (\omega^2 / \Delta^2) - \frac{1}{3}a [\Delta^2 / (\omega^2 + \Delta^2)]\} + O[(\theta'')^2], \quad (45)$$

$$\text{where } a = \theta'' \Psi'' (1 - \theta')^{-2} / \sigma(0) \quad (46)$$

$$\text{and } \Delta = |2\Sigma''(1 - \theta')^{-1}(1 - \frac{1}{2}a)|. \quad (47)$$

If  $a$  were 0, and if one identified  $\tau$  with  $[|2\Sigma''| / (1 - \theta')]^{-1}$ , then Eqs. (45) and (8) would be of the same form. This relaxation time  $\tau$ , although it differs somewhat from that discussed in conjunction with Eq. (40), is not an unexpected result. It can be identified as the inverse of the imaginary part of the pole in the Green's function when the latter is simplified using (42b) and Eqs. (44). This pole corresponds to the renormalized energy of Bloch states which lie on the Fermi surface of the pure crystal with  $\epsilon^A = \epsilon^B = 0$ .

For  $a \neq 0$ , the last factor in Eq. (45) modifies the "quasi-Drude" behavior. The most interesting special case is when

$$\Delta \ll \omega_m. \quad (48)$$

The terms behaving like  $\omega^2 / \Delta^2$  will cause deviations in Eq. (45) from its Drude-like form at large frequencies; the Lorentzian term will be appreciable only for  $\omega \lesssim \Delta$ . Consequently both for  $\omega$  near 0 and  $\omega$  near  $\omega_m$ , the frequency dependence of  $\sigma'(\omega)$  differs from that in Eq. (8).

Finally, we consider the weak-scattering limit of Eq. (45) to show when Drude behavior can be obtained outside the usual limits of validity, i.e., Eq. (16). As  $\epsilon^A - \epsilon^B \rightarrow 0$ , the second correction term vanishes, but the first becomes

$$\frac{2}{3}a\omega^2 / \Delta^2 \rightarrow \frac{1}{3}(\Psi''\omega / \Phi'')(dg^0/dz)\omega / g^0|_{\mu_0}. \quad (49)$$

This term can be interpreted as the product of the relative changes in  $\Phi''$  and in  $g^0$  over an interval of width  $\omega$ . It depends only on the pure-crystal

characteristics. If it is small for  $\omega < \omega_m$ , then in this weak-scattering approximation

$$\sigma'(\omega) = \sigma(0)\Delta^2(\omega^2 + \Delta^2)^{-1}.$$

Furthermore, in this limit Eq. (45) reduces to Eq. (8), because

$$\Delta \approx |2\Sigma''| = 2\pi x(1-x)(\epsilon^A - \epsilon^B)^2 g^0(\mu^0) = \tau^{-1},$$

as seen from Eqs. (15) and (23). Thus for the Fermi energy in a smooth part of the band and for a weakly scattering random potential, the Boltzmann equation may justifiably be extrapolated far beyond its usual limit [Eq. (16)].

#### V. DISCUSSION AND NUMERICAL EXAMPLES

In this section the results of the previous discussions will be briefly summarized and numerically illustrated at  $T = 0$ .

A simple cubic tight-binding dispersion relation  $\epsilon(k)$  is adopted,<sup>4</sup>

$$\epsilon(k) = -\frac{1}{3}W(\cos ak_x + \cos ak_y + \cos ak_z), \quad (50)$$

where  $W$  is the half-band width and  $a$  is the unit-cell dimension. This band shape is convenient because Eqs. (27) and (28) can be expressed simply in terms of Bessel function integrals<sup>11, 13</sup> and numerically evaluated.<sup>14</sup> We choose the bandwidth  $2W = 10$  eV and the unit-cell dimension = 2 Å. While these numbers are arbitrary, the parameters are given definite values so our results can be quantitatively illustrated. The critical points of Eq. (50) are at  $E_0 = -E_3 = -5$  eV and  $E_1 = -E_2 = -1.67$  eV.

The alloy is described by  $x$  the concentration of A atoms, and  $\epsilon^A - \epsilon^B$  the scattering strength. The energy origin is defined by  $\epsilon^A = -\epsilon^B > 0$ .  $\epsilon^A - \epsilon^B$  is assumed to range from 0.05 to 2.5 eV in the examples considered here. Then  $\Sigma''$  will vary from about  $10^{-4}$  to  $10^{-1}$  eV. This gives a mean free path from  $10^3$  to  $10^0$   $\mu$  and thus includes "optical" free paths  $c\tau$  of 10–50  $\mu$ , which is typical of most alloys.

Some of the scattering strengths considered lie outside the limits of the weak-scattering theory, but they all satisfy the condition that  $|\Sigma - \bar{\epsilon}|$  is less than the bandwidth. Consequently, the general statements made in Sec. IV are valid here. In view of the comparatively large scattering strengths considered, deviations from the rigid-band theory will be apparent, thus justifying the use of a more general approach like the CPA to the alloy problem. These deviations will be illustrated for both  $n_1$  and  $\sigma'(\omega)$ .

The quantity  $n_1$ , defined in Eq. (27), is of particular importance in optical experiments, for it completely characterizes  $\sigma'(\omega)$  for frequencies larger than 0.1 eV, as shown in Eq. (31). In

addition, it is proportional to the square of the plasma frequency

$$\omega_p^2 = n_1 e^2 / m \epsilon_\infty, \quad (51)$$

where  $\epsilon_\infty$  denotes the contribution of the interband transitions to the dielectric constant and, finally, it plays a role in the  $f$ -sum rule [Eq. (32)].

In Fig. 1, the quantity  $N_1 = n_1 \Omega_c$ , where  $\Omega_c$  = unit-cell volume, is plotted against the impurity concentration  $x$ . The effective number of carriers per site,  $N_1$ , may be compared to the electron concentration per site  $c$ . Because the volume  $\Omega_c$  of the sample is assumed constant, the alloying effects on  $N_1$  determine those on  $n_1$ . Shown in Fig. 1 are two families of curves corresponding to  $c = 0.2$  and  $c = 0.5$ . In each curve the value of  $\epsilon^A - \epsilon^B$  is held constant. The endpoints of each curve, corresponding to the same pure crystals, are identical. In the virtual-crystal limit, when  $\epsilon^A - \epsilon^B$  is small compared to the bandwidth, the band and hence the Fermi level shifts rigidly. Thus  $n_1$  is a constant in  $x$ , as shown for both elec-

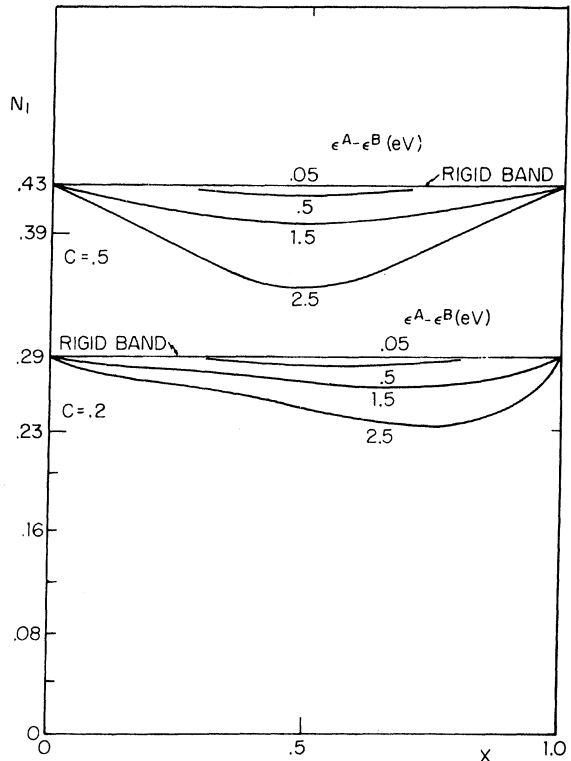


FIG. 1. Effective number of carriers per site  $N_1$  versus impurity concentration  $x$  for electron concentrations per site of  $c = 0.2$  and  $0.5$  and for several scattering strengths  $\epsilon^A - \epsilon^B$ .  $N_1$  is measured in units of  $(\frac{1}{2}a)^2 \frac{1}{5} W$  where  $a$  is the unit-cell dimension in Å and  $W$  is the half-band width in eV.

tron concentrations when  $\epsilon^A - \epsilon^B = 0.05$  eV. As the scattering parameter increases to 0.5 eV a "Nordheim" dependence on  $x$  appears;  $N_1$  is a quadratic function of  $x$ . For still larger  $\epsilon^A - \epsilon^B = 2.5$  eV, deviations from the right-band straight line and the quadratic  $x$  dependence are apparent for both  $c = 0.2$  and 0.5, although in the latter case, because  $c = 0.5$  corresponds to a half-filled band, the curves are all symmetric about  $x = 0.5$ . The origin of the asymmetry for  $c = 0.2$  and  $\epsilon^A - \epsilon^B = 2.5$  eV can be easily understood. For this case, the Fermi level lies in the bottom half of the band ( $\mu = -0.90$  eV at  $c = 0.2$ ,  $x = 0.9$ ); but for  $x > 0.5$  this region of the band corresponds to the strongly distorted impurity region.<sup>2</sup> Consequently, for  $x$  near 1, the deviation of  $N_1$  from its rigid-band behavior is expected to be more apparent than for  $x$  near 0.

Although these results are model dependent, they imply, contrary to what has sometimes been suggested,<sup>15</sup> that for typical scattering strengths in alloys, the  $x$  dependence of  $n_1$  is appreciable and may be observed in high-frequency ( $\omega \gg 1$ ) measurements of  $\sigma''$  [see Eq. (31)]. On the basis of the  $f$ -sum rule, it is sometimes argued that for large  $\omega$ ,  $\sigma''(\omega)$  is proportional to the number of electrons per unit volume, a quantity clearly independent of alloying. However, the "high" frequencies considered here are still below the onset of interband transitions, and Eq. (32) is the appropriate single-band sum rule. The quantity  $n_1$  which is dependent on the alloy potential thus appears in  $\sigma''(\omega)$ . To understand why optical constants are sensitive to alloying, it must be observed that  $(\omega\tau)^{-1}$ , however small, is not a small parameter of the problem, nor is it a particularly relevant one. More explicitly, the effects of alloying are contained in  $\sigma(\omega)$  as renormalizations in the electron energy and as shifts in the Fermi energy. This can be verified, for example, from Eq. (35). The condition  $\omega\tau \gg 1$  is not sufficient to make these effects vanish. It may be added independently of these results, some experimental evidence for the  $x$  dependence of  $\sigma''$  at high frequencies has been reported for Au-Ag alloys.<sup>16</sup>

We next consider the quantity  $\sigma'(\omega)$  and determine its frequency dependence for several choices of the parameters  $\mu$  and  $\epsilon^A - \epsilon^B$  and for fixed  $x = 0.1$ . The purpose of this discussion will be to compare the results obtained using a specific-band model Eq. (50) with the general formal results obtained in Sec. IV. To study  $\sigma'(\omega)$  we consider a more convenient quantity  $\tau(\omega)$ , simply related to  $\sigma'(\omega)$  by the equation

$$\sigma'(\omega) = \sigma(0) \{1 + [\omega\tau(\omega)]^2\}^{-1}. \quad (52)$$

The frequency dependence of  $\tau(\omega)$  reflects direct-

ly the difference between Eq. (38) and the Drude formula [Eq. (8)] in which  $\tau$  is frequency independent. Furthermore,  $\tau(\omega)$  does not vary rapidly over many orders of magnitude, as does the quantity  $\sigma'(\omega)$ ; consequently, it is advantageous to consider it rather than the real part of the conductivity itself.

In Fig. 2 is plotted  $\tau^{-1}(\omega)$  for  $x = 0.1$ ,  $\epsilon^A - \epsilon^B = 0.05$  eV. This represents the case of very weak scattering and therefore the imaginary part of  $\Sigma$ .  $\Sigma''(E - i\omega)$  is proportional to the pure-crystal density of states as shown in the insert. For this weakly scattering alloy  $\Sigma''$  assumes values less than  $10^{-3}$  eV. Critical points in the pure-crystal density of states are evident in  $\Sigma''$  and are denoted by  $M_0$ ,  $M_1$ ,  $M_2$ , and  $M_3$  corresponding to the energies  $E_0$ ,  $E_1$ ,  $E_2$ , and  $E_3$  listed above. In the high-frequency region, which includes nearly the entire frequency interval shown,  $\sigma'(\omega)$  can be easily obtained from  $\tau(\omega)$  by the equation  $\sigma'(\omega) = \sigma(0) [\omega\tau(\omega)]^{-2}$ . The two curves shown in Fig. 2 correspond to two Fermi energies 1.5 and 2.5 eV. These two energies are shown in the insert to indicate their relative positions in the band. For the second Fermi energy,  $\tau^{-1}(\omega)$  is nearly constant up to  $\omega = 0.5$  eV; it shows some structure beyond this and starts to rapidly decrease until it becomes zero at  $\omega = 10$  eV. (Figure 2 does not include frequencies this large.) It appears that Eq. (8) is a good approximation for  $\omega < 0.5$  eV, a fair one for  $\omega < 2.5$  eV, and a poor one thereafter when the absorption drops off very rapidly becoming zero at exactly 10 eV.

This behavior was predicted in the discussion in Sec. IV. Using Eq. (41), it is clear that the singular behavior in  $\Phi''(z - \Sigma)$  and in  $\Sigma''$  at energies  $E_c$  will be reflected in  $\sigma'(\omega)$  at frequencies  $|\mu - E_c|$ . Because  $\Phi''$  is very smooth,<sup>13</sup> the energies  $E_c$  will correspond to singularities in  $\Sigma''$  only. These occur at  $1$  eV =  $|\mu - E_2|$  and at  $2.5$  eV =  $|\mu - E_3|$ . These frequencies are indicated by arrows in Fig. 2. Beyond  $2.5$  eV  $\tau^{-1}(\omega)$  and hence  $\sigma'(\omega)$  rapidly decrease because both  $\Sigma''$  and  $\Phi''$  vanish for  $E > E_3$ . The integration region in Eq. (41) may then be replaced by  $(\mu - \omega, E_3 - \omega)$ , which does not increase with  $\omega$ . For frequencies equal to the bandwidth, the absorptive part of  $\sigma(\omega)$  becomes identically zero; thus,  $\tau^{-1}(\omega)$  must also vanish. The low-frequency ( $\omega \lesssim 0.5$  eV) behavior, in contrast to the high-frequency behavior, is Drude-like as Eq. (45) suggests for the special case of slowly varying  $\Sigma$  and  $\Phi$  in the interval  $(\mu - \omega, \mu + \omega)$ . The conditions for the validity of Eq. (45) are clearly satisfied for  $\omega \lesssim 0.5$  eV, as may be seen from the plot of  $\Sigma''$  in Fig. 2. Furthermore in this weak-scattering limit for low frequencies, the "correction" terms in Eq. (45) to the Drude fre-

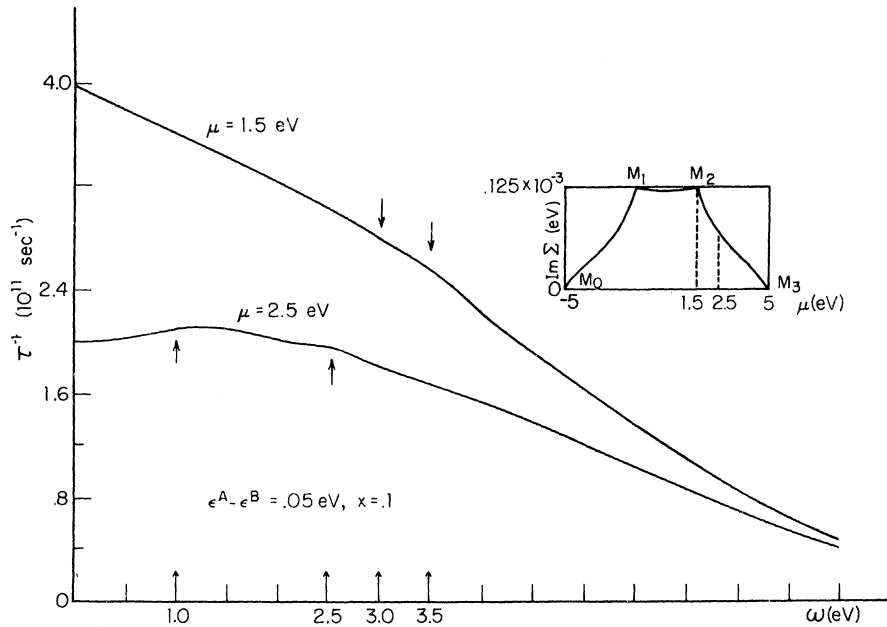


FIG. 2. Inverse relaxation time  $\tau^{-1}(\omega)$  versus  $\omega$  [see Eq. (52)] in the weak-scattering limit for Fermi energies  $\mu = 1.5$  and  $2.5$  eV and  $x = 0.1$ . The two arrows on each curve indicate frequencies  $|\mu - E_c|$ , where  $E_c$  is a critical-point energy corresponding to  $M_1$  and  $M_2$  ( $\mu = 1.5$ ), and  $M_3$  and  $M_4$  ( $\mu = 2.5$ ). These critical points are shown in the insert, which plots the imaginary part of the electron self-energy versus  $\mu$ .

quency dependence are negligible.

For the Fermi energy at  $\mu = 1.5$  eV, the low-frequency behavior is not frequency independent as in the previous case. This deviation from Drude-like behavior at low frequencies is a consequence of the fact that  $\mu = 1.5$  eV nearly coincides with the critical energy  $E_2 = 1.67$  eV. Correspondingly,  $\Sigma''$  varies too rapidly even at low frequencies to make any approximation as in Eqs. (42a) and (42b). It appears then, that dramatic deviations from the Drude formula (8) are expected when the Fermi level is close to critical points in the pure-crystal band.

We turn now to a moderately strongly scattering alloy. If  $\epsilon^A - \epsilon^B$  is increased to  $2.5$  eV for  $x = 0.1$ , the weak-scattering results of Fig. 2 must be modified. The imaginary part of the self-energy, as shown in the insert of Fig. 3, is no longer proportional to the unperturbed density of states. Critical points are no longer apparent and the band edges have shifted somewhat. A peak near the top of the band corresponds to increased damping in the impurity region. Although  $\Sigma''$  has increased in magnitude relative to the case of  $\epsilon^A - \epsilon^B = 0.05$  eV, it is still small compared to nearly all  $\omega$  in Fig. 3. While  $\tau^{-1}(\omega)$  is between three and four

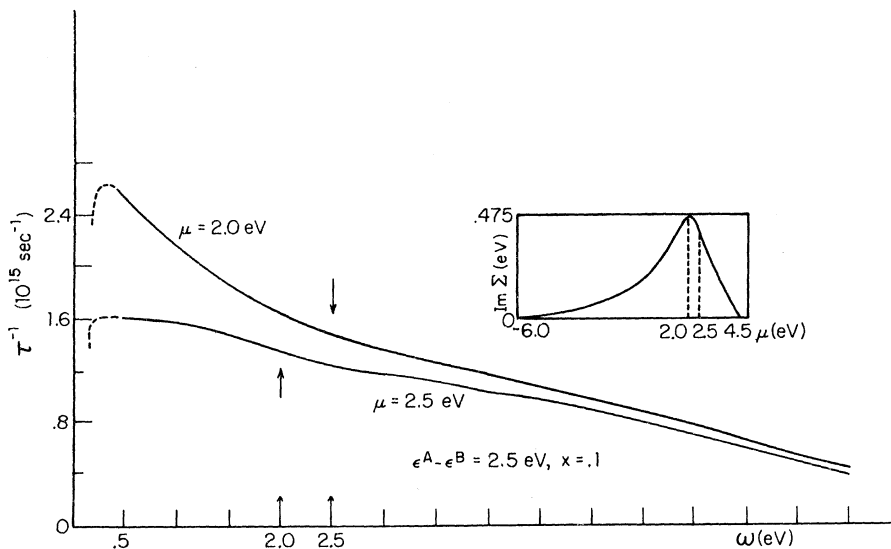


FIG. 3. The inverse relaxation time  $\tau^{-1}(\omega)$  versus  $\omega$  for two moderately strongly scattering alloys having Fermi energies  $\mu = 2.0$  and  $2.5$  eV and  $x = 0.1$ . The arrows indicate frequencies  $|\mu - E_c|$  where  $E_c$  is the upper-band edge. The insert plots the imaginary part of the electron self-energy versus  $\mu$ .

orders of magnitude higher than in the previous example, its general behavior is not very different. The two curves shown correspond to  $\mu = 2$  eV and 2.5 eV. They appear to be very similar except for frequencies less than 1.5 eV. Here for  $\mu = 2.5$  eV,  $\tau^{-1}(\omega)$  is only slightly  $\omega$  dependent, whereas for  $\mu = 2$  eV,  $\tau^{-1}(\omega)$  decreases with  $\omega$ . In the region of the higher  $\mu$ ,  $\Sigma''(E)$  varies linearly with  $E$ . However, for  $\mu = 2$  eV,  $\Sigma''$  varies more rapidly since 2 eV nearly coincides with the peak in  $\Sigma''$  as shown in the insert in Fig. 3. Equation (45) is valid for the Fermi energy at 2.5 eV away from any sharp structure in  $\Sigma''$ , but not for the Fermi energy at 2 eV which is close to a maximum in  $\Sigma''$ . Not shown in detail here is the behavior of  $\tau^{-1}(\omega)$  for very low frequencies. For both choices of  $\mu$  it appears to increase very rapidly from  $\omega = 0$ . This behavior may be qualitative-

ly associated with the first correction term in the last factor of Eq. (45). Although there appears no obvious physical reason for this behavior, its experimental implications are significant: The dc or low-frequency ac determinations of the relaxation time will give results different from the "optical" relaxation time, unless the scattering is weak, in which case the effect is negligible, as borne out numerically and theoretically [using Eq. (45) in the weak-scattering limit].

#### ACKNOWLEDGMENTS

The authors are grateful to Professor H. Ehrenreich for informing us of the experimental results of J. Rivory, which in part motivated our calculations. In addition, we wish to thank J. Rivory and F. Abelès for making their data available before publication.

---

\*Work supported in part by Grant No. GP-8019 of the National Science Foundation and the Advanced Research Projects Agency.

<sup>†</sup>Present address: Institute of Solid State Physics, Czechoslovak Academy of Sciences, Prague, Czechoslovakia.

<sup>1</sup>R. Kubo, J. Phys. Soc. Japan 12, 570 (1957).

<sup>2</sup>B. Velický, S. Kirkpatrick, and H. Ehrenreich, Phys. Rev. 175, 747 (1968).

<sup>3</sup>B. Velický, Phys. Rev. 184, 614 (1969).

<sup>4</sup>N. F. Mott and H. Jones, *The Theory of the Properties of Metals and Alloys* (Dover, New York, 1958), Chaps. 2 and 3.

<sup>5</sup>A. Lonke and A. Ron, in *Proceedings of the International Colloquium of Optical Properties and Electronic Structure of Metals and Alloys, Paris, 1965* (Wiley, New York, 1966).

<sup>6</sup>K. Yamada, Progr. Theoret. Phys. (Kyoto) 28, 299 (1962).

<sup>7</sup>A simple formula for  $\tau$  in the dilute limit may also be given. We treat the weak-scattering case for simplicity.

<sup>8</sup>We let  $\hbar = 1$ . The symbol  $\hat{}$  will denote operators. Primes will denote the real part of a complex number, double primes the imaginary part.

<sup>9</sup>L. Nordheim, Ann. Physik 9, 607 (1931).

<sup>10</sup>R. E. Peierls, *Quantum Theory of Solids* (Clarendon Oxford, 1955), p. 141.

<sup>11</sup>P. Soven, Phys. Rev. 156, 809 (1967); 178, 1136 (1969).

<sup>12</sup>The functions  $\Phi$  and  $\phi$  are related by  $\phi = d\Phi/dz$ . Thus for  $T = 0$ , Eq. (34) reduces to  $n = \pi^{-1} \Phi''(\mu^0 - i0)$ .

<sup>13</sup>K. Liebermann Levin, B. Velický, and H. Ehrenreich, Bull. Am. Phys. Soc. 14, 320 (1968).

<sup>14</sup>T. Wolfram and J. Callaway, Phys. Rev. 130, 2207 (1963).

<sup>15</sup>E. A. Stern, Phys. Rev. 144, 545 (1966).

<sup>16</sup>J. Rivory (private communication).